

# Design, synthesis and biological evaluation of novel trimethylpyrazine-2-carboxyloxy-cinnamic acids as potent cardiovascular agents†

Cite this: *Med. Chem. Commun.*, 2014, 5, 711

Hongfei Chen,<sup>a</sup> Guoning Li,<sup>a</sup> Peng Zhan,<sup>a</sup> Hong Li,<sup>b</sup> Shouxun Wang<sup>b</sup> and Xinyong Liu<sup>\*a</sup>

A series of novel trimethylpyrazine-2-carboxyloxy-cinnamic acids and esters were designed, synthesized and evaluated for their inhibitory effect on adenosine diphosphate (ADP)-induced platelet aggregation *in vitro* and also assayed for their protective effect against hydrogen peroxide (H<sub>2</sub>O<sub>2</sub>)-induced oxidative damage on Ea.hy926 cells. The results showed that many compounds exhibited high activity in one or both of the assays, of which, compound **F10** displayed the highest protective effect on the proliferation of the damaged Ea.hy926 cells (EC<sub>50</sub> = 1.7 μM), presenting almost 40 times higher potency than that of lipoic acid, and compound **F3** was the most active anti-platelet aggregation agent with IC<sub>50</sub> = 9.6 μM, comparable to that of clopidogrel. The structure–activity relationships of these compounds were also discussed.

Received 19th January 2014  
Accepted 10th March 2014

DOI: 10.1039/c4md00022f

www.rsc.org/medchemcomm

## Introduction

Cardiovascular diseases (CVDs) such as ischemic heart disease and stroke are the leading causes of death in the world.<sup>1</sup> Advances in pathophysiologic research have revealed that CVDs are caused by pathological states such as redox imbalance (oxidative stress), endothelial dysfunction, endothelial inflammation, and excessive vascular remodeling.<sup>2</sup>

Although the mechanisms underlying endothelial dysfunction are complicated and multifactorial, much evidence indicated that abnormally high levels of reactive oxygen species (ROS) may have a vital role in this phenomenon.<sup>3</sup>

ROS include hydrogen peroxide (H<sub>2</sub>O<sub>2</sub>), peroxynitrite (ONOO<sup>-</sup>), superoxide anions (O<sub>2</sub><sup>•-</sup>), hydroxyl radicals (HO<sup>•</sup>) and nitric oxide (NO<sup>•</sup>), which are created as part of normal cellular metabolism and defense systems.<sup>4</sup> Low levels of ROS are crucial for the redox homeostasis and various cellular signaling pathways and regulate fundamental cell activities including cellular growth, differentiation, proliferation and apoptosis.<sup>5–7</sup> At high concentrations, ROS leads to oxidative stress, which causes cell injury and death and contributes to the pathogenesis of atherosclerosis.<sup>8</sup>

Under normal conditions, the endothelium prevents platelets from interacting with the vessel wall by synthesizing platelet inhibitors, such as prostaglandin I<sub>2</sub> and NO, and shielding the subendothelial adhesive proteins from the platelets' contact.<sup>9</sup> When the endothelial cell lining is injured, platelets rapidly adhere to the exposed subendothelial matrix and adhesive proteins such as von Willebrand factor, collagen and fibrinogen.<sup>10</sup> Subsequent platelet activation results in the recruitment of additional platelets and then leads to aggregation to form a stable platelet plug.<sup>11,12</sup>

Ligustrazine (tetramethylpyrazine, TMP) is one of the alkaloids isolated from the Chinese herb, Chuanxiong. Ligustrazine has been routinely used to treat patients with coronary vascular diseases. It is reported that ligustrazine showed significant inhibition on shear-induced platelet aggregation and calcium channels in the platelet membrane.<sup>13,14</sup> In recent studies, ligustrazine is found to increase the production of NO in human umbilical vein endothelial cells (HUVECs) and had an immunomodulatory effect on HUVECs stimulated with TNF-α by downregulating the expression of 1 intercellular adhesion molecule and 60 heat shock proteins.<sup>15</sup> These results suggested that ligustrazine protects the endothelium *via* inhibition of immunological reactions.<sup>16</sup> Ligustrazine could also attenuate oxidative damage and apoptosis and ameliorate the down-regulation of superoxide dismutase (SOD) activity.<sup>17,18</sup>

Cinnamic acid and some of its derivatives (*e.g.* ferulic acid) (Fig. 1) are components of plants such as soybeans, peanuts and coffee, and they have been reported to display anti-oxidative properties. It is believed that cinnamic acids are potential scavengers of free radicals (such as O<sub>2</sub><sup>•-</sup>) and other oxidative species, which is one of the mechanisms for antioxidant

<sup>a</sup>Department of Medicinal Chemistry, Key Laboratory of Chemical Biology (Educational Ministry of China), School of Pharmaceutical Sciences, Shandong University, No. 44 Wenhua Road, Jinan 250012, China. E-mail: xinyongl@sdu.edu.cn

<sup>b</sup>Department of Biological Chemistry and Molecular Biology, School of Medicine, Weifang Medical University, No. 7166 Baotongxi Road, Weifang 261053, China

† Electronic supplementary information (ESI) available. See DOI: 10.1039/c4md00022f

potential of oilseeds.<sup>19,20</sup> Ozagrel (Fig. 1), a derivative of cinnamic acid, is reported to be a highly selective thromboxane (TXA<sub>2</sub>) synthase inhibitor. It is clinically used for the treatment of acute cerebral thrombosis and prevention of postoperative cerebral ischaemia, by precluding the TXA<sub>2</sub> induced platelet aggregation.<sup>21,22</sup>

In our previous work, it was found that some of ligustrazine metabolites, such as 3,5,6-trimethylpyrazine-2-carboxylic acid, displayed moderate activity on lowering the level of serum cholesterol and low density lipoprotein *in vivo* (Fig. 1).

Inspired by the structural characteristics and the drug-like properties of cinnamic acid and in continuation of our work, we conjugated the ligustrazinyloxy group with a cinnamic acid group to obtain a novel series of trimethylpyrazine-2-carboxyloxy-cinnamic acids (see Fig. 2), in the hope of getting novel ligustrazine derivatives with high anti-oxidative activity or anti-platelet aggregation activity. It is a further objective of this paper to understand the structure–activity relationships and to afford information through diversified molecular modification of ligustrazine.

## Results and discussion

### Chemistry

A convenient synthetic route to title compounds is shown in Scheme 1. In this approach 3,5,6-trimethylpyrazine-2-carboxylic acid (2), previously synthesized by oxidation of ligustrazine (1) with potassium permanganate, was reacted with oxalyl chloride in dichloromethane in an ice bath for 10 min, to obtain 3,5,6-trimethylpyrazine-2-carbonyl chloride (3), which was used for the next step directly. Compounds **F(1–10)** were synthesized from 3 by reaction with cinnamic acids, and followed by esterification to afford the corresponding trimethylpyrazine-2-carboxyloxy-cinnamic acid esters **F'(1–10)**. Cinnamic acids with different substituents at the phenyl group were prepared according to the Knoevenagel condensation,<sup>23</sup> depicted in

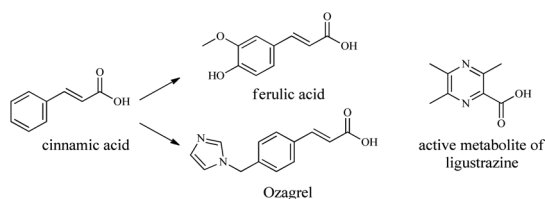


Fig. 1 Structure of cinnamic acid, ferulic acid, ozagrel and 3,5,6-trimethylpyrazine-2-carboxylic acid.

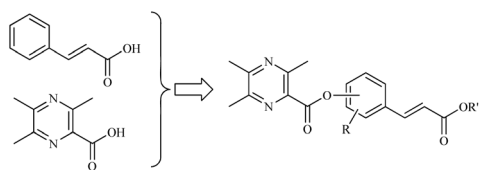
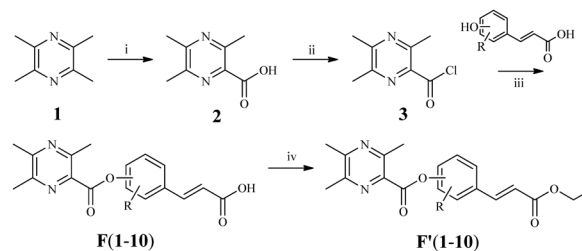
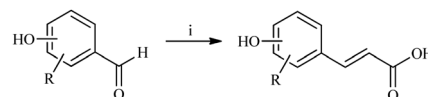


Fig. 2 Design of trimethylpyrazine-2-carboxyloxy-cinnamic acids.



Scheme 1 Reagents and conditions: (i) KMnO<sub>4</sub>, H<sub>2</sub>O, 35 °C, 24 h, (ii) oxalyl chloride, anhydrous DCM, ice bath, 10 min, (iii) Et<sub>3</sub>N, anhydrous DCM, r.t., 1 h, and (iv) EtOH, SOCl<sub>2</sub>, reflux, 12 h.



Scheme 2 Preparation of the hydroxyl cinnamic acids. Reagents and conditions: (i) malonic acid, pyridine, cat. piperidine, 120 °C, 1.5 h.

Table 1 Structures of the synthesized compounds

Compound	Structure	Compound	Structure
<b>F1</b>		<b>F'1</b>	
<b>F2</b>		<b>F'2</b>	
<b>F3</b>		<b>F'3</b>	
<b>F4</b>		<b>F'4</b>	
<b>F5</b>		<b>F'5</b>	
<b>F6</b>		<b>F'6</b>	
<b>F7</b>		<b>F'7</b>	
<b>F8</b>		<b>F'8</b>	
<b>F9</b>		<b>F'9</b>	
<b>F10</b>		<b>F'10</b>	

Scheme 2. All the newly synthesized compounds (Table 1) were structurally confirmed by IR, <sup>1</sup>H-NMR and MS.

### Biological results

**Anti-platelet activity.** The newly synthesized compounds, ligustrazine and some cinnamic acids/ethyl esters were tested for their inhibition against rabbit platelet aggregation *in vitro*;<sup>24</sup> ozagrel and clopidogrel were used as control drugs. The results, expressed as the aggregation inhibition rate (AIR) and IC<sub>50</sub>, are summarized in Table 2.

As shown in Table 2, 4-OH-cinnamic acid, 4-OH-ethyl cinnamate, 2-OH-cinnamic acid and ethyl ferulate displayed moderate anti-platelet aggregation activity (IC<sub>50</sub> = 74.8, 130.4, 115.8 and 193.2 μM, respectively), while ligustrazine possessed weaker anti-platelet aggregation activity (IC<sub>50</sub> = 265.3 μM). The corresponding ligustrazine–cinnamic acids/ethyl esters (**F1**, **F'1**, **F3** and **F'4**) exhibited enhanced activity (IC<sub>50</sub> = 37.8, 24.4, 9.6 and 58.4 μM, respectively), indicating that the conjugation is an effective approach to obtain more potent compounds.

Among all the synthesized compounds, **F'1**, **F2**, **F3**, **F5**, **F'7** and **F'9** were the most potent platelet aggregation inhibitors with IC<sub>50</sub> values 24.4, 26.4, 9.6, 41.8, 28.2 and 37.5 μM, respectively, much more active than that of ozagrel (IC<sub>50</sub> = 144.1 μM), but slightly lower than that of clopidogrel (IC<sub>50</sub> = 7.6 μM).

In the case of compounds derived from monosubstituted cinnamic acid (**F1**, **F2** and **F3**), a clear order of

trimethylpyrazine-2-carboxyloxy position at the phenyl group of cinnamic acids for antiplatelet activity was observed as the following: *ortho*-position > *meta*-position > *para*-position. In the *ortho*-substituted series **F(3, 6–8)**, compounds containing a methoxyl or chloro group at the phenyl ring of cinnamic acids **F(6–8)** displayed reduced anti-platelet activities (IC<sub>50</sub> = 57.2, 133.8, and 49.0 μM, respectively) compared to monosubstituent compound **F3**. The structure–activity relationship (SAR) analysis provided important information for further molecular optimization.

It is noteworthy that the activity of some compounds is not concentration dependent, such as for **F1**, **F'1** and **F2**, whose AIR value decreased with higher concentrations. Since the platelet aggregation is a rather complicated process, it is not clear which factor affected the aggregation in the assay. A possible reason is that high concentrations of those compounds activated the platelets and induced the aggregation.

The possible anti-platelet aggregation mechanisms of the synthesized ligustrazine derivatives are (1) that they are probably TXA<sub>2</sub> synthase inhibitors, considering that they contain a similar cinnamic acid moiety with ozagrel and (2) that the ligustrazine moiety played a role in inhibiting calcium channels in the platelet membrane. Further molecular biological study is underway to confirm the mechanism of these compounds.

**Protective effect on damaged Ea.hy926 cells.** Setting liponic acid and butylated hydroxyanisole (BHA) as the positive

Table 2 The IC<sub>50</sub> for inhibition of platelet aggregation

Compound	AIR 100 μM	AIR 50 μM	AIR 25 μM	AIR 12.5 μM	IC <sub>50</sub> <sup>a</sup> (μM)
<b>F1</b>	25.3%	41.7%	53.3%	64.3%	37.8 ± 9.3
<b>F'1</b>	20.5%	32.2%	39.1%	68.0%	24.4 ± 8.5
<b>F2</b>	8.2%	28.0%	38.5%	73.4%	26.4 ± 3.9
<b>F'2</b>	69.4%	59.6%	62.2%	25.1%	35.8 ± 15.2
<b>F3</b>	17.2%	53.8%	54.8%	32.9%	9.6 ± 5.2
<b>F'3</b>	42.4%	39.0%	16.6%	11.8%	110.2 ± 17.2
<b>F4</b>	73.2%	46.2%	22.8%	60.6%	44.6 ± 7.3
<b>F'4</b>	64.4%	49.9%	37.2%	31.0%	58.4 ± 5.8
<b>F5</b>	75.2%	59.8%	53.5%	21.6%	41.8 ± 4.2
<b>F'5</b>	39.7%	32.2%	20.6%	22.3%	143.0 ± 13.7
<b>F6</b>	74.5%	37.0%	38.1%	30.0%	57.2 ± 6.4
<b>F'6</b>	61.7%	44.4%	36.9%	26.3%	67.1 ± 4.1
<b>F7</b>	40.9%	34.1%	35.1%	16.5%	133.8 ± 19.1
<b>F'7</b>	47.0%	18.7%	32.6%	84.2%	28.2 ± 4.2
<b>F8</b>	59.8%	48.8%	46.5%	43.4%	49.0 ± 3.9
<b>F'8</b>	60.7%	72.9%	73.9%	70.5%	195.8 ± 30.4
<b>F9</b>	52.1%	51.2%	17.4%	12.0%	82.3 ± 5.5
<b>F'9</b>	59.5%	55.9%	47.2%	44.0%	37.5 ± 4.5
<b>F10</b>	53.6%	44.5%	25.0%	32.1%	84.6 ± 6.2
<b>F'10</b>	58.4%	37.9%	36.4%	22.0%	77.4 ± 5.8
Ozagrel	36.8%	25.0%	4.8%	6.4%	144.1 ± 12.1
Clopidogrel	94.5%	92.3%	77.6%	86.9%	7.6 ± 2.3
4-OH-cinnamic acid	54.5%	53.2%	29.9%	17.2%	74.8 ± 3.7
4-OH-ethyl cinnamate	37.9%	25.5%	16.4%	5.8%	130.4 ± 8.9
2-OH-cinnamic acid	42.9%	30.5%	21.4%	10.8%	115.8 ± 5.5
Ethyl ferulate	26.5%	17.9%	11.5%	4.0%	193.2 ± 11.2
Ligustrazine	19.6%	15.3%	8.6%	3.4%	265.3 ± 14.5

<sup>a</sup> IC<sub>50</sub>: concentration of compound required to achieve 50% inhibition on aggregation of rabbit platelets.

Table 3 The EC<sub>50</sub> values for protection on damaged Ea.hy926 cells and P% at different concentrations of the compounds

Compound	P% (100 μM)	P% (50 μM)	P% (25 μM)	P% (12.5 μM)	EC <sub>50</sub> <sup>a</sup> (μM)
<b>F1</b>	93.2%	74.1%	46.6%	34.2%	38.0 ± 2.2
<b>F'1</b>	96.1%	62.6%	58.8%	42.7%	34.9 ± 3.7
<b>F2</b>	103.0%	75.3%	64.3%	61.6%	24.0 ± 2.1
<b>F'2</b>	47.0%	39.5%	34.2%	27.9%	92.6 ± 2.8
<b>F3</b>	80.1%	64.9%	61.8%	45.7%	36.7 ± 3.5
<b>F'3</b>	40.9%	36.9%	17.8%	9.6%	108.4 ± 4.1
<b>F4</b>	55.4%	49.1%	40.3%	38.7%	69.4 ± 4.9
<b>F'4</b>	71.6%	69.7%	53.3%	52.4%	38.6 ± 1.7
<b>F5</b>	216.3%	159.6%	128.1%	41.3%	8.8 ± 1.1
<b>F'5</b>	117.0%	89.0%	60.1%	26.4%	29.9 ± 1.4
<b>F6</b>	52.2%	23.7%	26.0%	6.9%	95.2 ± 4.2
<b>F'6</b>	11.0%	33.7%	62.5%	64.9%	36.1 ± 1.6
<b>F7</b>	18.0%	31.6%	-52.1%	39.7%	115.3 ± 4.9
<b>F'7</b>	39.9%	20.7%	16.9%	-57.6%	137.7 ± 5.2
<b>F8</b>	79.2%	62.9%	45.0%	21.7%	48.6 ± 2.2
<b>F'8</b>	46.2%	27.8%	23.4%	15.9%	104.6 ± 4.4
<b>F9</b>	163.0%	96.6%	24.0%	5.7%	34.7 ± 1.5
<b>F'9</b>	-47.0%	-13.6%	20.9%	96.6%	21.4 ± 1.5
<b>F10</b>	601.4%	284.8%	271.1%	92.8%	2.2 ± 1.1
<b>F'10</b>	375.3%	210.8%	207.0%	75.7%	1.7 ± 0.9
Lipoic acid	58.1%	48.7%	-12.3%	30.5%	68.0 ± 5.9
BHA	43.4%	28.0%	22.6%	17.2%	111.4 ± 5.2
3-OH-4-OCH <sub>3</sub> -cinnamic acid	81.9%	62.9%	36.8%	34.9%	29.3 ± 2.3
3,5-diOCH <sub>3</sub> -4-OH-ethyl cinnamate	69.1%	32.0%	24.9%	4.9%	67.2 ± 2.1
Caffeic acid	155.6%	149.5%	108.5%	16.7%	12.6 ± 1.8
Ethyl caffeate	146.9%	134.8%	88.4%	80.4%	11.6 ± 1.0
Ligustrazine	40.9%	22.1%	13.6%	11.4%	83.4 ± 4.1

<sup>a</sup> EC<sub>50</sub>: concentration of compound required to achieve 50% protection of Ea.hy926 cells from H<sub>2</sub>O<sub>2</sub> induced cytotoxicity, as determined by the MTT method.

control drugs, all the synthesized compounds, ligustrazine and some cinnamic acids/ethyl esters, were also tested for their protective effect on the Ea.hy926 cells damaged by hydrogen peroxide.<sup>25,26</sup> Table 3 revealed the proliferation rate (P%) at different concentrations and 50% effective concentration for protecting damaged Ea.hy926 cells of newly synthesized compounds.

As shown in Table 3, 3-OH-4-OCH<sub>3</sub>-cinnamic acid, 3,5-diOCH<sub>3</sub>-4-OH-ethyl cinnamate, caffeic acid (**F10**) and ethyl caffeate (**F'10**) displayed moderate to high anti-platelet aggregation activity (IC<sub>50</sub> = 29.3, 67.2, 12.6 and 11.6 μM, respectively), while ligustrazine possessed mild anti-platelet aggregation activity (IC<sub>50</sub> = 83.4 μM). The corresponding ligustrazine-cinnamic acids/ethyl esters (**F5**, **F'9**, **F10** and **F'10**) exhibited enhanced activity (IC<sub>50</sub> = 8.8, 21.4, 2.2 and 1.7 μM, respectively).

From the obtained results, it was observed that some of the trimethylpyrazine-2-carboxyloxy-cinnamic acids/ethyl esters protected the proliferation of injured Ea.hy926 cells with commensurable or higher potency compared to control drugs lipoic acid or BHA (EC<sub>50</sub> = 68.0 μM, 111.4 μM, respectively). Among all the trimethylpyrazine-2-carboxyloxy-cinnamic acid and esters, **F2**, **F5**, **F'5**, **F'9**, **F10**, and **F'10** displayed remarkable anti-oxidative activity (EC<sub>50</sub> = 24.0, 8.8, 29.9, 21.4, 2.2, and 1.7 μM, respectively). Particularly, the compound **F'10** presented almost 40 times higher potency than lipoic acid.

Among compounds **F(1, 4, 9, 10)** and **F'(1, 4, 9, 10)** substituted with trimethylpyrazine-2-carboxyloxy groups at

the *para* position of the cinnamic acids, **F10** and **F'10** (EC<sub>50</sub> = 2.2 and 1.7 μM, respectively) with the hydroxyl group at the 3 position of the benzene ring showed better protective effects than compounds **F1** and **F'1** (EC<sub>50</sub> = 38.0 and 34.9 μM), which may be attributed to the anti-oxidative effect of the hydroxyl group. From the proliferation rate presented in Table 3, it also can be found that the potencies of compounds **F10** and **F'10** were concentration dependent, reaching the maximum value (P% = 601.4%, 375.3%, respectively) at 100 μM, whereas compounds **F4** and **F'4** containing a methoxyl group at the 3 position of the phenyl group did not give desirable potencies. Among compounds **F(2, 5)** and **F'(2, 5)** substituted with trimethylpyrazine-2-carboxyloxy groups at the *meta* position of the cinnamic acid, **F5** and **F'5** with the methoxyl group at the 5 position of the phenyl ring showed enhanced protective effects (EC<sub>50</sub> = 8.8 and 29.9 μM, respectively) than compounds **F2** and **F'2** (EC<sub>50</sub> = 24.0 and 92.6 μM, respectively).

As listed in the table, the activity of most compounds' is concentration dependent, except for **F'6**, **F7** and **F'9**, whose P% value decreased with higher concentration. The possible reason is that high concentrations of these compounds exhibited toxicity rather than protection to the cells.

The mechanism of the synthesized compounds' anti-oxidative activity may be attributed to the free radical-scavenging effect of both ligustrazine and cinnamic acids/ethyl esters, the conjugation of which led to a synergic effect.

## Conclusion

In conclusion, a series of novel trimethylpyrazine-2-carboxyloxy-cinnamic acids were designed, synthesized and biologically evaluated for their inhibitory activities against the platelet aggregation, and their protective effect on the damaged Ea.hy926 cell proliferation. The results showed that some compounds exhibited high activity in one or both of the assays, of which compound **F10** displayed the highest protective effect on the proliferation of the damaged Ea.hy926 cells ( $EC_{50} = 1.7 \mu\text{M}$ ), and compound **F3** was the most active anti-platelet aggregation agent with  $IC_{50} = 9.6 \mu\text{M}$ , demonstrating the potential values in further development of cardiovascular agents. The structure-activity relationship was discussed in detail. In addition, the molecular research of these novel compounds is underway. Further studies are ongoing in our laboratories and will be reported in due course.

## Experimental

The melting points of the compounds were metered on a micromelting point apparatus. Infrared spectra were recorded with a Nexus 470 FT-IR Spectrometer.  $^1\text{H}$  NMR spectra were determined using a Bruker Avance (400 MHz) NMR-spectrometer in the indicated solvents. Chemical shifts are expressed in  $\delta$  units and TMS as the internal reference. Mass spectra were recorded with an LC Autosampler Device: Standard G1313A instrument. TLC was performed on silica gel GF254 for TLC (Merck) and spots were visualized by iodine vapors or by irradiation with UV light (254 nm). Flash column chromatography was performed on a column packed with silica gel 60 (230–400 mesh). Solvents were of reagent grade and, when necessary, were purified and dried by standard methods. The concentration of the reaction solutions involved the use of a rotary evaporator at reduced pressure. The yields were calculated using the last step reaction.

### General procedure for the preparation of the compounds **F1–10**

To an aqueous solution of 2,3,5,6-tetramethylpyrazine (0.1 mol) was added potassium permanganate (0.4 mol). The reaction mixture was stirred at  $35^\circ\text{C}$  for 24 h to give the intermediate 3,5,6-trimethylpyrazine-2-carboxylic acid. Oxalyl chloride (2 mmol) was added to the dichloromethane (10 mL, anhydrous) solution of 3,5,6-trimethylpyrazine-2-carboxylic acid (2 mmol) in an ice bath. When the addition was completed with further stirring for 10 min, the solvent and redundant oxalyl chloride were removed under reduced pressure to obtain 3,5,6-trimethylpyrazine-2-carbonyl chloride.

Cinnamic acids with different substituents at the phenyl group were prepared according to the Knoevenagel condensation. To the solution of hydroxybenzaldehyde (2.0 mmol) in pyridine were added malonic acid (2.4 mmol) and piperidine. The mixture was refluxed at  $120^\circ\text{C}$  for 1.5 h. Upon completion of the reaction, the mixture was diluted with ethyl acetate (100 mL) and washed with 0.1 N HCl solution. The organic layer was dried with  $\text{Na}_2\text{SO}_4$ , filtered and concentrated under reduced pressure to afford cinnamic acids.

Cinnamic acid (2 mmol) was added into the dichloromethane solution of 3,5,6-trimethylpyrazine-2-carbonyl chloride (2 mmol) obtained in the above step at room temperature; triethylamine (4 mmol) was added to the mixture which was then stirred at  $25^\circ\text{C}$  for 1 h (checked by TLC). The solvent was removed and the residue was dissolved in ethyl acetate (100 mL), washed with water and brine, successively. The organic layer was dried with  $\text{Na}_2\text{SO}_4$ , filtered and concentrated under reduced pressure to afford the crude product. The final product was purified by flash column chromatography and recrystallization from ethyl acetate.

**(E)-3-(4-((3,5,6-Trimethylpyrazine-2-carbonyloxy)phenyl)acrylic acid (F1)**. White needle crystals, yield: 63%, mp:  $212\text{--}214^\circ\text{C}$ .  $^1\text{H-NMR}$  (400 MHz,  $\text{CDCl}_3$ ,  $\delta$  ppm): 12.46 (s, 1H, COOH), 7.82 (d, 2H, Ar-H,  $J = 8.4$  Hz), 7.66 (d, 1H, Ar-CH=C,  $J = 16.0$  Hz), 7.36 (d, 2H, Ar-H,  $J = 8.4$  Hz), 6.58 (d, 1H, C=CH-C=O,  $J = 16.0$  Hz), 2.72 (s, 3H,  $\text{CH}_3$ ), 2.57 (s, 3H,  $\text{CH}_3$ ), 2.55 (s, 3H,  $\text{CH}_3$ ). IR (KBr,  $\text{cm}^{-1}$ ): 3400 (OH), 2925 ( $\text{CH}_3$ ), 1743, 1693 (C=O), 1628 (C=C), 1599, 1583, 1506 (C=N, C=C), 1164 (C-O). ESI-MS:  $313.3$  ( $\text{M} + \text{H}^+$ ), calcd for  $\text{C}_{17}\text{H}_{16}\text{N}_2\text{O}_4$  312.32.

**(E)-3-(3-((3,5,6-Trimethylpyrazine-2-carbonyloxy)phenyl)acrylic acid (F2)**. Yellow powder, yield: 54%, mp:  $208\text{--}210^\circ\text{C}$ .  $^1\text{H-NMR}$  (400 MHz,  $\text{CDCl}_3$ ,  $\delta$  ppm): 12.48 (s, 1H, COOH), 7.68–7.60 (m, 3H, Ar-H, Ar-CH=C), 7.54 (t, 1H, Ar-H,  $J = 7.8$  Hz), 7.36 (dd, 1H, Ar-H,  $J_1 = 1.5$  Hz,  $J_2 = 7.9$  Hz), 6.64 (d, 1H, C=CH-C=O,  $J = 16.0$  Hz), 2.73 (s, 3H,  $\text{CH}_3$ ), 2.57 (s, 3H,  $\text{CH}_3$ ), 2.55 (s, 3H,  $\text{CH}_3$ ). IR (KBr,  $\text{cm}^{-1}$ ): 3450 (OH), 2966, 2852 ( $\text{CH}_3$ ), 1736, 1692 (C=O), 1631 (C=C), 1580, 1539 (C=N, C=C), 1172 (C-O). ESI-MS:  $313.4$  ( $\text{M} + \text{H}^+$ ), calcd for  $\text{C}_{17}\text{H}_{16}\text{N}_2\text{O}_4$  312.32.

**(E)-3-(2-((3,5,6-Trimethylpyrazine-2-carbonyloxy)phenyl)acrylic acid (F3)**. Light yellow needle crystals, yield: 57%, mp:  $204\text{--}206^\circ\text{C}$ .  $^1\text{H-NMR}$  (400 MHz,  $\text{CDCl}_3$ ,  $\delta$  ppm): 12.48 (s, 1H, COOH), 7.94 (d, 1H, Ar-H,  $J = 7.8$  Hz), 7.67 (d, 1H, Ar-CH=C,  $J = 15.6$  Hz), 7.56–7.53 (m, 1H, Ar-H), 7.42–7.38 (m, 2H, Ar-H), 6.75 (d, 1H, C=CH-C=O,  $J = 15.6$  Hz), 2.71 (s, 3H,  $\text{CH}_3$ ), 2.58 (s, 3H,  $\text{CH}_3$ ), 2.50 (s, 3H,  $\text{CH}_3$ ). IR (KBr,  $\text{cm}^{-1}$ ): 3450 (OH), 2980, 2929 ( $\text{CH}_3$ ), 1733, 1692 (C=O), 1627 (C=C), 1577, 1543 (C=N, C=C), 1166 (C-O). ESI-MS:  $313.4$  ( $\text{M} + \text{H}^+$ ), calcd for  $\text{C}_{17}\text{H}_{16}\text{N}_2\text{O}_4$  312.32.

**(E)-3-(3-Methoxy-4-((3,5,6-trimethylpyrazine-2-carbonyloxy)phenyl)acrylic acid (F4)**. White needle crystals, yield: 61%, mp:  $214\text{--}218^\circ\text{C}$ .  $^1\text{H-NMR}$  (400 MHz,  $\text{CDCl}_3$ ,  $\delta$  ppm): 12.44 (s, 1H, COOH), 7.63 (d, 1H, Ar-CH=C,  $J = 15.6$  Hz), 7.56 (s, 1H, Ar-H), 7.34 (d, 1H, Ar-H,  $J = 7.8$  Hz), 7.30 (d, 1H, Ar-H,  $J = 7.8$  Hz), 6.65 (d, 1H, C=CH-C=O,  $J = 16.2$  Hz), 3.85 (s, 3H,  $\text{OCH}_3$ ), 2.70 (s, 3H,  $\text{CH}_3$ ), 2.56 (s, 3H,  $\text{CH}_3$ ), 2.51 (s, 3H,  $\text{CH}_3$ ).  $^{13}\text{C-NMR}$  (400 MHz,  $\text{CDCl}_3$ ,  $\delta$  ppm): 119.94, 121.87, 124.21, 133.62, 137.93, 141.17, 143.73, 147.73, 150.10, 151.48, 155.96, 165.11 (–COO–), 168.11 (–COO–).  $^{13}\text{C-NMR}$  (400 MHz,  $\text{CDCl}_3$ ,  $\delta$  ppm): 21.51 (– $\text{CH}_3$ ), 22.38 (– $\text{CH}_3$ ), 22.61 (– $\text{CH}_3$ ), 56.19 (– $\text{OCH}_3$ ), 112.25, 119.94, 121.87, 123.62, 133.62, 137.93, 141.17, 143.73, 150.10, 151.48, 151.80, 155.96, 163.69 (–COO–), 168.11 (–COO–). IR (KBr,  $\text{cm}^{-1}$ ): 3422 (OH), 2924, 2852 ( $\text{CH}_3$ ), 1745, 1696 (C=O), 1630 (C=C), 1591 (C=N, C=C), 1152 (C-O). ESI-MS:  $343.5$  ( $\text{M} + \text{H}^+$ ), calcd for  $\text{C}_{18}\text{H}_{18}\text{N}_2\text{O}_5$  342.35. HRMS:  $m/z$  calcd for  $\text{C}_{18}\text{H}_{18}\text{N}_2\text{O}_5$  [ $\text{M} + \text{H}^+$ ] 343.1290, found 343.1288.

**(E)-3-(4-Methoxy-3-((3,5,6-trimethylpyrazine-2-carbonyl)oxy)phenyl)acrylic acid (F5).** White needle crystals, yield: 64%, mp: 202–204 °C. <sup>1</sup>H-NMR (400 MHz, CDCl<sub>3</sub>, δ ppm): 12.36 (s, 1H, COOH), 7.68–7.61 (m, 3H, Ar-H, Ar-CH=C), 7.24 (d, 1H, Ar-H, *J* = 8.4 Hz), 6.48 (d, 1H, C=CH-C=O, *J* = 16.2 Hz), 3.84 (s, 3H, OCH<sub>3</sub>), 2.71 (s, 3H, CH<sub>3</sub>), 2.57–2.49 (m, 6H, CH<sub>3</sub> × 2). IR (KBr, cm<sup>-1</sup>): 3488 (OH), 2957, 2927, 2848 (CH<sub>3</sub>), 1753, 1720 (C=O), 1636 (C=C), 1610 (C=N, C=C), 1161 (C-O). ESI-MS: 343.5 (M + H)<sup>+</sup>, calcd for C<sub>18</sub>H<sub>18</sub>N<sub>2</sub>O<sub>5</sub> 342.35.

**(E)-3-(5-Chloro-2-((3,5,6-trimethylpyrazine-2-carbonyl)oxy)phenyl)acrylic acid (F6).** White needle crystals, yield: 89%, mp: 229–233 °C. <sup>1</sup>H-NMR (400 MHz, CDCl<sub>3</sub>, δ ppm): 12.79 (s, 1H, COOH), 8.06 (d, 1H, Ar-CH=C, *J* = 2 Hz), 7.63–7.58 (m, 2H, Ar-H), 7.50 (d, 1H, Ar-H, *J* = 8.7 Hz), 6.88 (d, 1H, C=CH-C=O, *J* = 16.0 Hz), 2.72 (s, 3H, CH<sub>3</sub>), 2.62–2.48 (m, 6H, CH<sub>3</sub> × 2). IR (KBr, cm<sup>-1</sup>): 3429 (OH), 2960, 2925, 2854 (CH<sub>3</sub>), 1739, 1696 (C=O), 1629 (C=C), 1571, 1541 (C=N, C=C), 1159 (C-O). ESI-MS: 347.3 (M + H)<sup>+</sup>, calcd for C<sub>17</sub>H<sub>15</sub>ClN<sub>2</sub>O<sub>4</sub> 346.76.

**(E)-3-(4-Methoxy-2-((3,5,6-trimethylpyrazine-2-carbonyl)oxy)phenyl)acrylic acid (F7).** White needle crystals, yield: 84%, mp: 210–212 °C. <sup>1</sup>H-NMR (400 MHz, CDCl<sub>3</sub>, δ ppm): 12.32 (s, 1H, COOH), 7.88 (d, 1H, Ar-H, *J* = 8.8 Hz), 7.59 (s, 1H, Ar-CH=C, *J* = 16.0 Hz), 7.04 (d, 1H, Ar-H, *J* = 2.5 Hz), 6.99 (dd, 1H, Ar-H, *J*<sub>1</sub> = 2.6 Hz, *J*<sub>2</sub> = 8.8 Hz), 6.61 (d, 1H, C=CH-C=O, *J* = 16.0 Hz), 3.83 (s, 3H, OCH<sub>3</sub>), 2.72 (s, 3H, CH<sub>3</sub>), 2.58 (s, 3H, CH<sub>3</sub>), 2.51 (s, 3H, CH<sub>3</sub>). IR (KBr, cm<sup>-1</sup>): 3478 (OH), 2956, 2927 (CH<sub>3</sub>), 1761, 1720 (C=O), 1636 (C=C), 1610 (C=N, C=C), 1161 (C-O). ESI-MS: 343.4 (M + H)<sup>+</sup>, calcd for C<sub>18</sub>H<sub>18</sub>N<sub>2</sub>O<sub>5</sub> 342.35.

**(E)-3-(5-Methoxy-2-((3,5,6-trimethylpyrazine-2-carbonyl)oxy)phenyl)acrylic acid (F8).** White powder, yield: 81%, mp: 213–215 °C. <sup>1</sup>H-NMR (400 MHz, CDCl<sub>3</sub>, δ ppm): 12.48 (s, 1H, COOH), 7.61 (d, 1H, Ar-CH=C, *J* = 16.2 Hz), 7.44 (s, 1H, Ar-H), 7.33 (d, 1H, Ar-H, *J* = 9 Hz), 7.10 (m, 1H, Ar-H), 6.80 (d, 1H, C=CH-C=O, *J* = 16.2 Hz), 3.84 (s, 3H, OCH<sub>3</sub>), 2.70 (s, 3H, CH<sub>3</sub>), 2.57–2.44 (m, 6H, CH<sub>3</sub> × 2). IR (KBr, cm<sup>-1</sup>): 3442 (OH), 2977, 2924, 2836 (CH<sub>3</sub>), 1732, 1693 (C=O), 1632 (C=C), 1582, 1541 (C=N, C=C), 1161 (C-O). ESI-MS: 343.4 (M + H)<sup>+</sup>, calcd for C<sub>18</sub>H<sub>18</sub>N<sub>2</sub>O<sub>5</sub> 342.35.

**(E)-3-(3,5-Dimethoxy-4-((3,5,6-trimethylpyrazine-2-carbonyl)oxy)phenyl)acrylic acid (F9).** White needle crystals, yield: 82%, mp: 228–232 °C. <sup>1</sup>H-NMR (400 MHz, CDCl<sub>3</sub>, δ ppm): 12.44 (s, 1H, COOH), 7.62 (d, 1H, Ar-CH=C, *J* = 16.0 Hz), 7.19 (s, 2H, Ar-H), 6.70 (d, 1H, C=CH-C=O, *J* = 16.0 Hz), 3.83 (s, 6H, OCH<sub>3</sub> × 2), 2.70 (s, 3H, CH<sub>3</sub>), 2.56–2.50 (m, 6H, CH<sub>3</sub> × 2). <sup>13</sup>C-NMR (400 MHz, CDCl<sub>3</sub>, δ ppm): 21.53 (–CH<sub>3</sub>), 22.38 (–CH<sub>3</sub>), 22.51 (–CH<sub>3</sub>), 56.75 (–OCH<sub>3</sub> × 2), 105.74 (Ar-carbon × 2), 120.44, 129.65, 133.49, 138.04, 144.15, 150.17, 151.33, 152.36 (Ar-carbon × 2), 155.92, 163.41 (–COO–), 168.07 (–COO–). IR (KBr, cm<sup>-1</sup>): 3429 (OH), 2941, 2847 (CH<sub>3</sub>), 1755, 1706 (C=O), 1641 (C=C), 1595, 1541 (C=N, C=C), 1167 (C-O). ESI-MS: 373.3 (M + H)<sup>+</sup>, calcd for C<sub>19</sub>H<sub>20</sub>N<sub>2</sub>O<sub>6</sub> 372.37. HRMS: *m/z* calcd for C<sub>19</sub>H<sub>20</sub>N<sub>2</sub>O<sub>6</sub> [M + H]<sup>+</sup> 373.1396, found 373.1394; [M + Na]<sup>+</sup> 395.1213, found 395.1214.

**(E)-3-(3-Hydroxy-4-((3,5,6-trimethylpyrazine-2-carbonyl)oxy)phenyl)acrylic acid (F10).** White needle crystals, yield: 84%, mp: 220–222 °C. <sup>1</sup>H-NMR (400 MHz, CDCl<sub>3</sub>, δ ppm): 12.45 (s, 1H, COOH), 7.62 (d, 1H, Ar-CH=C, *J* = 16.2 Hz), 7.19 (s, 2H, Ar-H),

6.69 (d, 1H, C=CH-C=O, *J* = 15.6 Hz), 5.35 (s, 2H, OH), 2.71 (s, 3H, CH<sub>3</sub>), 2.56–2.50 (m, 6H, CH<sub>3</sub> × 2). <sup>13</sup>C-NMR (400 MHz, CDCl<sub>3</sub>, δ ppm): 21.47 (–CH<sub>3</sub>), 22.32 (–CH<sub>3</sub>), 22.67 (–CH<sub>3</sub>), 117.20, 119.56, 123.29, 128.20, 133.60, 138.31, 139.11, 143.74, 149.64, 149.91, 151.47, 155.64, 162.75 (–COO–), 172.47 (–COO–). IR (KBr, cm<sup>-1</sup>): 3470 (OH), 2966, 2852 (CH<sub>3</sub>), 1736, 1692 (C=O), 1631 (C=C), 1580, 1539 (C=N, C=C), 1172 (C-O). ESI-MS: 329.5 (M + H)<sup>+</sup>, calcd for C<sub>17</sub>H<sub>16</sub>N<sub>2</sub>O<sub>5</sub> 328.11. HRMS: *m/z* calcd for C<sub>17</sub>H<sub>16</sub>N<sub>2</sub>O<sub>5</sub> [M + H]<sup>+</sup> 329.1137, found 329.1132.

#### General procedure for the preparation of the compounds F'(1–10)

To an icy solution of the ligustrazinacyl-cinnamic acids (10 mmol) in ethanol (30 mL) was added thionyl chloride (0.5 mL) dropwise. The reaction mixture was refluxed for 24 h to give the corresponding crude ethyl cinnamate. Upon completion of the reaction, the solvent was removed and the residue was diluted with ethyl acetate, and washed with water and brine, successively. The organic layer was dried with Na<sub>2</sub>SO<sub>4</sub>, filtered and concentrated under reduced pressure to afford the crude product. The final product was purified by flash column chromatography and recrystallization from *n*-hexane.

**(E)-4-(3-Ethoxy-3-oxoprop-1-en-1-yl)phenyl-3,5,6-trimethylpyrazine-2-carboxylate (F'1).** White needle crystals, yield: 81%, mp: 77–80 °C. <sup>1</sup>H-NMR (400 MHz, CDCl<sub>3</sub>, δ ppm): 7.86 (d, 2H, Ar-H, *J* = 8.6 Hz), 7.72 (d, 1H, Ar-CH=C, *J* = 16.0 Hz), 7.37 (d, 2H, Ar-H, *J* = 8.6 Hz), 6.68 (d, 1H, C=CH-C=O, *J* = 16.0 Hz), 4.24 (q, 2H, OCH<sub>2</sub>, *J* = 7.0 Hz), 2.72 (s, 3H, CH<sub>3</sub>), 2.57 (s, 3H, CH<sub>3</sub>), 2.55 (s, 3H, CH<sub>3</sub>), 1.30 (t, 3H, CH<sub>3</sub>, *J* = 7.1 Hz). IR (KBr, cm<sup>-1</sup>): 3063 (C=C-H), 2988, 2929 (CH<sub>3</sub>), 1747, 1712 (C=O), 1642 (C=C), 1601, 1541, 1509 (C=N, C=C), 1169 (C-O). ESI-MS: 341.4 (M + H)<sup>+</sup>, calcd for C<sub>19</sub>H<sub>20</sub>N<sub>2</sub>O<sub>4</sub> 340.37.

**(E)-3-(3-Ethoxy-3-oxoprop-1-en-1-yl)phenyl-3,5,6-trimethylpyrazine-2-carboxylate (F'2).** White needle crystals, yield: 81%, mp: 87–91 °C. <sup>1</sup>H-NMR (400 MHz, CDCl<sub>3</sub>, δ ppm): 7.72–7.66 (m, 3H, Ar-H, Ar-CH=C), 7.55 (t, 1H, Ar-H, *J* = 7.9 Hz), 7.37 (dd, 1H, Ar-H, *J*<sub>1</sub> = 1.6 Hz, *J*<sub>2</sub> = 7.9 Hz), 6.74 (d, 1H, C=CH-C=O, *J* = 16.0 Hz), 4.23 (q, 2H, OCH<sub>2</sub>, *J* = 7.1 Hz), 2.73 (s, 3H, CH<sub>3</sub>), 2.57 (s, 3H, CH<sub>3</sub>), 2.55 (s, 3H, CH<sub>3</sub>), 1.30 (t, 3H, CH<sub>3</sub>, *J* = 7.1 Hz). IR (KBr, cm<sup>-1</sup>): 3061 (C=C-H), 2977, 2927 (CH<sub>3</sub>), 1731, 1716 (C=O), 1637 (C=C), 1604, 1583, 1541 (C=N, C=C), 1169 (C-O). ESI-MS: 341.4 (M + H)<sup>+</sup>, calcd for C<sub>19</sub>H<sub>20</sub>N<sub>2</sub>O<sub>4</sub> 340.37.

**(E)-2-(3-Ethoxy-3-oxoprop-1-en-1-yl)phenyl-3,5,6-trimethylpyrazine-2-carboxylate (F'3).** White needle crystals, yield: 81%, mp: 77–79 °C. <sup>1</sup>H-NMR (400 MHz, CDCl<sub>3</sub>, δ ppm): 7.97 (d, 1H, Ar-H, *J* = 7.8 Hz), 7.75 (d, 1H, Ar-CH=C, *J* = 16.2 Hz), 7.61–7.54 (m, 1H, Ar-H), 7.45–7.38 (m, 2H, Ar-H), 6.93 (d, 1H, C=CH-C=O, *J* = 16.1 Hz), 4.23 (q, 2H, OCH<sub>2</sub>, *J* = 7.2 Hz), 2.73 (s, 3H, CH<sub>3</sub>), 2.57–2.49 (m, 6H, CH<sub>3</sub> × 2), 1.30 (t, 3H, CH<sub>3</sub>, *J* = 7.2 Hz). <sup>13</sup>C-NMR (400 MHz, CDCl<sub>3</sub>, δ ppm): 14.54 (–CH<sub>3</sub>), 21.57 (–CH<sub>3</sub>), 22.39 (–CH<sub>3</sub>), 22.46 (–CH<sub>3</sub>), 60.25 (–OCH<sub>2</sub>–), 119.84, 121.38, 123.87, 127.22, 129.37, 131.96, 137.98, 140.42, 149.59, 150.18, 151.88, 156.25, 164.12 (–COO–), 166.52 (–COO–). IR (KBr, cm<sup>-1</sup>): 3080 (C=C-H), 2988, 2957 (CH<sub>3</sub>), 1745, 1705 (C=O), 1629 (C=C), 1601, 1577, 1541 (C=N, C=C), 1151 (C-O). ESI-MS: 341.4 (M + H)<sup>+</sup>, calcd for C<sub>19</sub>H<sub>20</sub>N<sub>2</sub>O<sub>4</sub> 340.37. HRMS: *m/z* calcd for

$C_{19}H_{20}N_2O_4$   $[M + H]^+$  341.1501, found 341.1496;  $[M + Na]^+$  363.1317, found 363.1315.

**(E)-4-(3-Ethoxy-3-oxoprop-1-en-1-yl)-2-methoxyphenyl-3,5,6-trimethylpyrazine-2-carboxylate (F'4).** White needle crystals, yield: 81%, mp: 107–110 °C.  $^1H$ -NMR (400 MHz,  $CDCl_3$ ,  $\delta$  ppm): 7.70 (d, 1H, Ar-CH=C,  $J = 16.0$  Hz), 7.61 (s, 1H, Ar-H), 7.38 (d, 1H, Ar-H,  $J = 8.2$  Hz), 7.31 (d, 1H, Ar-H,  $J = 8.2$  Hz), 6.77 (d, 1H, C=CH-C=O,  $J = 16.0$  Hz), 4.23 (q, 2H,  $OCH_2$ ,  $J = 7.1$  Hz), 3.85 (s, 3H,  $OCH_3$ ), 2.70 (s, 3H,  $CH_3$ ), 2.56 (s, 3H,  $CH_3$ ), 2.51 (s, 3H,  $CH_3$ ), 1.30 (t, 3H,  $CH_3$ ,  $J = 7.1$  Hz).  $^{13}C$ -NMR (400 MHz,  $CDCl_3$ ,  $\delta$  ppm): 14.65 (– $CH_3$ ), 21.49 (– $CH_3$ ), 22.35 (– $CH_3$ ), 22.55 (– $CH_3$ ), 56.59 (– $OCH_3$ ), 60.50 (– $OCH_2$ –), 112.60, 119.15, 122.17, 123.62, 133.88, 137.99, 141.39, 144.16, 150.06, 151.52, 151.72, 155.89, 163.67 (– $COO$ –), 166.66 (– $COO$ –). IR (KBr,  $cm^{-1}$ ): 3064 (C=C–H), 2983, 2928 ( $CH_3$ ), 1737, 1703 (C=O), 1676 (C=C), 1601, 1510 (C=N, C=C), 1158 (C–O). ESI-MS: 371.4 ( $M + H$ ) $^+$ , calcd for  $C_{20}H_{22}N_2O_5$  370.40. HRMS:  $m/z$  calcd for  $C_{20}H_{22}N_2O_5$   $[M + H]^+$  371.1608, found 371.1601;  $[M + Na]^+$  393.1422, found 393.1421.

**(E)-5-(3-Ethoxy-3-oxoprop-1-en-1-yl)-2-methoxyphenyl-3,5,6-trimethylpyrazine-2-carboxylate (F'5).** White needle crystals, yield: 54%, mp: 119–122 °C.  $^1H$ -NMR (400 MHz,  $CDCl_3$ ,  $\delta$  ppm): 7.74–7.61 (m, 3H, Ar-H, Ar-CH=C), 7.24 (d, 1H, Ar-H,  $J = 8.6$  Hz), 6.59 (d, 1H, C=CH-C=O,  $J = 16.0$  Hz), 4.23 (q, 2H,  $OCH_2$ ,  $J = 7.0$  Hz), 3.84 (s, 3H,  $OCH_3$ ), 2.71 (s, 3H,  $CH_3$ ), 2.57–2.50 (m, 6H,  $CH_3 \times 2$ ), 1.30 (t, 3H,  $CH_3$ ,  $J = 7.1$  Hz). IR (KBr,  $cm^{-1}$ ): 3064 (C=C–H), 2976, 2930 ( $CH_3$ ), 1741, 1705 (C=O), 1636 (C=C), 1611, 1512 (C=N, C=C), 1155 (C–O). ESI-MS: 371.5 ( $M + H$ ) $^+$ , calcd for  $C_{20}H_{22}N_2O_5$  370.40.

**(E)-4-Chloro-2-(3-ethoxy-3-oxoprop-1-en-1-yl)phenyl-3,5,6-trimethylpyrazine-2-carboxylate (F'6).** White needle crystals, yield: 75%, mp: 96–99 °C.  $^1H$ -NMR (400 MHz,  $CDCl_3$ ,  $\delta$  ppm): 8.09 (d, 1H, Ar-CH=C,  $J = 2.5$  Hz), 7.70–7.60 (m, 2H, Ar-H), 7.52 (d, 1H, Ar-H,  $J = 8.7$  Hz), 7.04 (d, 1H, C=CH-C=O,  $J = 16.2$  Hz), 4.18 (q, 2H,  $OCH_2$ ,  $J = 7.1$  Hz), 2.71 (s, 3H,  $CH_3$ ), 2.60–2.50 (m, 6H,  $CH_3 \times 2$ ), 1.30 (t, 3H,  $CH_3$ ,  $J = 7.1$  Hz). IR (KBr,  $cm^{-1}$ ): 3088 (C=C–H), 2994, 2981 ( $CH_3$ ), 1735, 1717 (C=O), 1634 (C=C), 1570, 1542 (C=N, C=C), 1180 (C–O). ESI-MS: 375.4 ( $M + H$ ) $^+$ , calcd for  $C_{19}H_{19}ClN_2O_4$  374.82.

**(E)-2-(3-Ethoxy-3-oxoprop-1-en-1-yl)-5-methoxyphenyl-3,5,6-trimethylpyrazine-2-carboxylate (F'7).** White needle crystals, yield: 80%, mp: 87–89 °C.  $^1H$ -NMR (400 MHz,  $CDCl_3$ ,  $\delta$  ppm): 7.70 (d, 1H, Ar-CH=C,  $J = 16.2$  Hz), 7.61 (s, 1H, Ar-H), 7.38 (d, 1H, Ar-H,  $J = 7.8$  Hz), 7.31 (d, 1H, Ar-H,  $J = 8.4$  Hz), 6.77 (d, 1H, C=CH-C=O,  $J = 15.6$  Hz), 4.23 (q, 2H,  $OCH_2$ ,  $J = 7.1$  Hz), 3.86 (s, 3H,  $OCH_3$ ), 2.70 (s, 3H,  $CH_3$ ), 2.56 (s, 3H,  $CH_3$ ), 2.51 (s, 3H,  $CH_3$ ), 1.30 (t, 3H,  $CH_3$ ,  $J = 7.1$  Hz). IR (KBr,  $cm^{-1}$ ): 3064 (C=C–H), 2976, 2930 ( $CH_3$ ), 1741, 1705 (C=O), 1636 (C=C), 1611, 1512 (C=N, C=C), 1155 (C–O). ESI-MS: 371.5 ( $M + H$ ) $^+$ , calcd for  $C_{20}H_{22}N_2O_5$  370.40.

**(E)-2-(3-Ethoxy-3-oxoprop-1-en-1-yl)-4-methoxyphenyl-3,5,6-trimethylpyrazine-2-carboxylate (F'8).** White needle crystals, yield: 80%, mp: 78–80 °C.  $^1H$ -NMR (400 MHz,  $CDCl_3$ ,  $\delta$  ppm): 7.69 (d, 1H, Ar-CH=C,  $J = 16.1$  Hz), 7.48 (s, 1H, Ar-H), 7.35 (d, 1H, Ar-H,  $J = 8.9$  Hz), 7.11 (dd, 1H, Ar-H,  $J_1 = 3.0$  Hz,  $J_2 = 8.9$  Hz), 6.97 (d, 1H, C=CH-C=O,  $J = 16.1$  Hz), 4.18 (q, 2H,  $OCH_2$ ,  $J = 7.1$  Hz), 3.84 (s, 3H,  $OCH_3$ ), 2.70 (s, 3H,  $CH_3$ ), 2.59–2.50 (m, 6H,  $CH_3 \times 2$ ), 1.33 (t, 3H,  $CH_3$ ,  $J = 7.1$  Hz). IR (KBr,  $cm^{-1}$ ): 3064

(C=C–H), 2981, 2963 ( $CH_3$ ), 1740, 1704 (C=O), 1635 (C=C), 1581, 1543 (C=N, C=C), 1157 (C–O). ESI-MS: 371.4 ( $M + H$ ) $^+$ , calcd for  $C_{20}H_{22}N_2O_5$  370.40.

**(E)-4-(3-Ethoxy-3-oxoprop-1-en-1-yl)-2,6-dimethoxyphenyl-3,5,6-trimethylpyrazine-2-carboxylate (F'9).** White needle crystals, yield: 75%, mp: 83–85 °C.  $^1H$ -NMR (400 MHz,  $CDCl_3$ ,  $\delta$  ppm): 7.68 (d, 1H, Ar-CH=C,  $J = 16.0$  Hz), 7.23 (s, 2H, Ar-H), 6.82 (d, 1H, C=CH-C=O,  $J = 16.0$  Hz), 4.23 (q, 2H,  $OCH_2$ ,  $J = 7.1$  Hz), 3.85 (s, 6H,  $OCH_3 \times 2$ ), 2.70 (s, 3H,  $CH_3$ ), 2.56–2.50 (m, 6H,  $CH_3 \times 2$ ), 1.30 (t, 3H,  $CH_3$ ,  $J = 7.1$  Hz).  $^{13}C$ -NMR (400 MHz,  $CDCl_3$ ,  $\delta$  ppm): 14.64 (– $CH_3$ ), 21.50 (– $CH_3$ ), 22.35 (– $CH_3$ ), 22.51 (– $CH_3$ ), 56.75 (– $OCH_3 \times 2$ ), 60.51 (– $OCH_2$ –), 105.89 (Ar-carbon  $\times 2$ ), 119.31, 129.84, 133.26, 138.03, 144.61, 150.14, 151.34, 152.38 (Ar-carbon  $\times 2$ ), 155.89, 163.39 (– $COO$ –), 166.68 (– $COO$ –). IR (KBr,  $cm^{-1}$ ): 3075 (C=C–H), 2977, 2925 ( $CH_3$ ), 1691 (C=O), 1633 (C=C), 1600, 1515 (C=N, C=C), 1156 (C–O). ESI-MS: 401.4 ( $M + H$ ) $^+$ , calcd for  $C_{21}H_{24}N_2O_6$  400.43. HRMS:  $m/z$  calcd for  $C_{21}H_{24}N_2O_6$   $[M + H]^+$  401.1706, found 401.1707;  $[M + Na]^+$  423.1521, found 423.1527.

**(E)-4-(3-Ethoxy-3-oxoprop-1-en-1-yl)-2-hydroxyphenyl-3,5,6-trimethylpyrazine-2-carboxylate (F'10).** White needle crystals, yield: 64%, mp: 90–92 °C.  $^1H$ -NMR (400 MHz,  $CDCl_3$ ,  $\delta$  ppm): 7.62 (d, 1H, Ar-CH=C,  $J = 16.2$  Hz), 7.19 (s, 2H, Ar-H), 6.69 (d, 1H, C=CH-C=O,  $J = 15.6$  Hz), 5.35 (s, 2H, OH), 4.23 (q, 2H,  $OCH_2$ ,  $J = 7.1$  Hz), 2.71 (s, 3H,  $CH_3$ ), 2.56–2.50 (m, 6H,  $CH_3 \times 2$ ), 1.30 (t, 3H,  $CH_3$ ,  $J = 7.1$  Hz).  $^{13}C$ -NMR (400 MHz,  $CDCl_3$ ,  $\delta$  ppm): 14.32 (– $CH_3$ ), 21.10 (– $CH_3$ ), 22.17 (– $CH_3$ ), 22.45 (– $CH_3$ ), 60.46 (– $OCH_2$ –), 116.56, 118.05, 122.46, 127.22, 133.79, 138.47, 139.82, 143.65, 149.74, 150.26, 152.89, 156.26, 163.14 (– $COO$ –), 167.02 (– $COO$ –). IR (KBr,  $cm^{-1}$ ): 3384.13 (OH), 3064 (C=C–H), 2976, 2930 ( $CH_3$ ), 1741, 1705 (C=O), 1636 (C=C), 1611, 1512 (C=N, C=C), 1155 (C–O). ESI-MS: 357.4 ( $M + H$ ) $^+$ , calcd for  $C_{19}H_{20}N_2O_6$  356.14. HRMS:  $m/z$  calcd for  $C_{19}H_{20}N_2O_6$   $[M + H]^+$  357.1449, found 357.1445;  $[M + Na]^+$  379.1267, found 379.1264.

#### Anti-platelet activity assay<sup>27</sup>

Rabbit blood was obtained using a cardiac puncture and transferred to a test tube containing 3.8% sodium citrate aqueous solution. Platelet-rich plasma (PRP) was obtained following blood sample centrifugation at 1000 rpm for 5 min. The PRP samples were again centrifuged at 3000 rpm for 15 min to obtain platelet-poor plasma (PPP), which was used as a reference solution in aggregation assays. The platelets of the precipitate were adjusted to the suitable number ( $3 \times 10^{11} L^{-1}$ ) for the aggregation assay. All platelet preparations were conducted at room temperature. 90  $\mu L$  PRP and 5  $\mu L$  sample solution (final concentration: 400, 200, 100, and 50  $\mu M$ ) was added into the microplate and incubated on 37 °C for 5 min. The microplate was put on an aggregometer and vibrated for 10 min, then monitored by measuring 570 nm transmission ( $A_0$ ). The monitoring took place every 30 s. After that 5  $\mu L$  ADP (work concentration: 5  $\mu M$ ) was added and 570 nm transmission was monitored every 30 s until it became stable ( $A$ ). The aggregation rate (AR) = (Abs PRP – Abs sample)/(Abs PRP – Abs PPP). The aggregation inhibition rate (AIR) =  $[1 - (AR_{\text{sample}}/AR_{\text{control}})] \times 100\%$ . Analysis of the derived data using a curve fitting software from OriginLab gave the  $IC_{50}$  values.

### Protective effect on damaged Ea.hy926 cells<sup>25,28</sup>

Ea.hy926 cells were seeded in a 96-well plate at a density of  $6 \times 10^3$  per well and allowed to grow to the desired confluence. The cells were pretreated with various concentrations of ligustrazine derivatives for 24 h, and then exposed to 150  $\mu\text{M}$   $\text{H}_2\text{O}_2$  for another 12 h. Control cells were incubated with a media containing an equivalent solvent amount without the test materials. The plate was incubated at 37 °C in a humidified 5%  $\text{CO}_2$  atmosphere. 12 hours later, 0.01 mL 3-(4,5-dimethylthiazol-2-yl)-2,5-diphenyltetrazolium bromide (MTT) solution (5 mg  $\text{mL}^{-1}$  in DMSO) was added to each well and then incubated for 4 h. Ligustrazine derivatives were dissolved in dimethyl sulfoxide (DMSO) and added into the wells (the final concentration of ligustrazine derivatives was to 100, 50, 25, and 12.5  $\mu\text{M}$ , and the DMSO content should never exceed 0.05%) and were incubated with cells for 24 h before the addition of  $\text{H}_2\text{O}_2$ . The supernatant was removed carefully by pipetting from wells without disturbing the attached cells and formazan crystals were solubilized by adding 200  $\mu\text{L}$  of DMSO to each well and shaken for 15 min. The absorbance at 570 nm was measured with a microplate reader, using wells without cells as the control. The proliferation rates of damaged Ea.hy926 cells were calculated by  $[\text{OD}_{570}(\text{compound}) - \text{OD}_{570}(\text{H}_2\text{O}_2)] / [\text{OD}_{570}(\text{control}) - \text{OD}_{570}(\text{H}_2\text{O}_2)] \times 100\%$ , which was then used to obtain  $\text{EC}_{50}$  values.

### Acknowledgements

The financial supports of this work by the National Key Projects of New Drugs R&D (2009ZX09103-117), Shandong Natural Science Foundation, Science and Technology Development Foundation of Shandong Province (2006GG2202063) are gratefully acknowledged.

### Notes and references

- 1 C. D. Mathers, T. Boerma and D. Ma Fat, *Br. Med. Bull.*, 2009, **92**, 7–32.
- 2 M. Maqsood, K. Yu Xiang and M. Bashir, *Oxid. Med. Cell. Longevity*, 1900, **2**, 259–269.
- 3 T. Münzel, T. Gori, R. M. Bruno and S. Taddei, *Eur. Heart J.*, 2010, **31**, 2741–2748.
- 4 J. M. Muller-Delp, A. N. Gurovich, D. D. Christou and C. Leeuwenburgh, *Microcirculation*, 2012, **19**, 19–28.
- 5 Y. S. Bae, H. Oh, S. G. Rhee and Y. D. Yoo, *Mol. Cells*, 2011, **32**, 491–509.
- 6 G. Aliev, Y. Li, H. H. Palacios and M. E. Obrenovich, *Recent Pat. Cardiovasc. Drug Discovery*, 2011, **6**, 222–241.
- 7 I. Olmez and H. Ozyurt, *Neurochem. Int.*, 2012, **60**, 208–212.
- 8 J. G. Park and G. T. Oh, *BMB Rep.*, 2011, **44**, 497–505.
- 9 B. S. Collier, *J. Thromb. Haemostasis*, 2011, **9**(suppl. 1), 374–395.
- 10 M. Ueno, M. Kodali, A. Tello-Montoliu and D. J. Angiolillo, *J. Atheroscler. Thromb.*, 2011, **18**, 431–442.
- 11 E. C. Lowenberg, J. C. Meijers and M. Levi, *Neth. J. Med.*, 2010, **68**, 242–251.
- 12 L. F. Brass, L. Zhu and T. J. Stalker, *Arterioscler., Thromb., Vasc. Biol.*, 2008, **28**, s43–s50.
- 13 F. Liao, *Clin. Hemorheol. Microcirc.*, 2000, **23**, 127–131.
- 14 F. Liao and L. Jiao, *Clin. Hemorheol. Microcirc.*, 2000, **22**, 167–168.
- 15 L. Feng, N. Ke, F. Cheng, Y. Guo, S. Li, Q. Li and Y. Li, *J. Surg. Res.*, 2011, **166**, 298–305.
- 16 H. J. Wu, J. Hao, S. Q. Wang, B. L. Jin and X. B. Chen, *Eur. J. Pharmacol.*, 2011, **674**, 365–369.
- 17 C. Gao, H. Peng, S. Wang and X. Zhang, *Burns*, 2012, **38**, 102–107.
- 18 C. Gao, Y. Liu, L. Ma, X. Zhang and S. Wang, *Burns*, 2012, **38**, 743–750.
- 19 P. K. Singh, R. Singh and S. Singh, *Physiol. Mol. Biol. Plants*, 2013, **19**, 53–59.
- 20 F. Song, H. Li, J. Sun and S. Wang, *J. Ethnopharmacol.*, 2013, **150**, 125–130.
- 21 K. Arii, H. Igarashi, T. Arii and Y. Katayama, *Life Sci.*, 2002, **71**, 2983–2994.
- 22 S. I. Park, D. K. Jang, Y. M. Han, Y. Y. Sunwoo, M. S. Park, Y. A. Chung, L. S. Maeng, R. Im, M. W. Kim, S. S. Jeun and K. S. Jang, *J. Biomed. Biotechnol.*, 2010, **2010**, 893401.
- 23 H. Chen, G. Li, P. Zhan and X. Liu, *Eur. J. Med. Chem.*, 2011, **46**, 5609–5615.
- 24 B. Bednar, C. Condra, R. J. Gould and T. M. Connolly, *Thromb. Res.*, 1995, **77**, 453–463.
- 25 X. C. Cheng, X. Y. Liu, W. F. Xu, X. L. Guo and Y. Ou, *Bioorg. Med. Chem.*, 2007, **15**, 3315–3320.
- 26 X. C. Cheng, X. Y. Liu, W. F. Xu, X. L. Guo, N. Zhang and Y. N. Song, *Bioorg. Med. Chem.*, 2009, **17**, 3018–3024.
- 27 B. Walkowiak, A. Keszy and L. Michalec, *Thromb. Res.*, 1997, **87**, 95–103.
- 28 Y. K. Wang and Z. Q. Huang, *Pharmacol. Res.*, 2005, **52**, 174–182.